Twist-4 contributions to the hadron structure functions

Jianwei Qiu
High Energy Physics Division, Argonne National Laboratory, Argonne, Illinois 60439
*and Institute for Theoretical Physics, State University of New York, Stony Brook, New York 11794**
(Received 10 January 1990)

We present a new method for calculating the twist-4 contributions to the hadron structure functions. This new method leads to a clear space-time picture of twist-4 short-distance contributions and makes manifest the preservation of the underlying gauge invariance. The use of our new method results in a significant reduction in labor relative to past calculations of higher-twist contributions. In our new approach, the twist-4 short-distance contributions to the hadronic structure functions arise from the complete imaginary part of a photon-parton forward-scattering amplitude, and, hence, they can be given a simple parton-model interpretation. Possible tests of such twist-4 contributions are also discussed.

I. INTRODUCTION

The parton model[1] has provided us with a simple and intuitive description of scaling phenomena of many high-energy scattering processes. With the leading-twist $\log Q^2$ corrections, the QCD-improved parton model[2] gives even better predictions of high-energy experimental data. Furthermore, the twist-4, or inverse-power $1/Q^2$ corrections in inelastic processes will make precision tests of QCD, the strong-interaction theory. This problem has been discussed by many authors.[3-6] Three complete and consistent analyses of twist-4, or inverse-power $1/Q^2$ corrections to deeply inelastic lepton-hadron scattering have been carried out. Jaffe and Soldate[4] (JS) used operator-product-expansion (OPE) methods to relate the inverse-power corrections to the target matrix elements of certain classes of twist-4 local operators. Ellis, Furmanski, and Petronzio[5] (EFP) used graphical methods to express the inverse-power corrections in terms of certain generalized quark-gluon correlation functions. Jaffe[6] later recasted the result of OPE analysis in the language of the parton model. All these analyses are technically very complicated. Particularly, it is not clear after a very long and complicated derivation that the twist-4 short-distance contributions to the hadron structure functions can be related to some simple physical proton-parton processes. In this paper, we shall introduce a new method (a new physical concept—the special propagator) to separate the different-twist contributions of a Feynman diagram. This new method leads to a clear space-time picture of twist-4 short-distance contributions and makes manifest the preservation of underlying gauge invariance. Using this method, we shall give another complete analysis of the inverse-power corrections. Our new approach not only reproduces the result of EFP, but also gives the result of simple parton-model interpretation. In particular, the use of our new method results in a significant reduction in labor relative to past calculations of higher-twist contributions.

In deeply inelastic lepton-hadron scattering, the strong interaction is governed by the hadronic tensor $W^{\mu\nu}(p,q)$ where p is the total momentum of the target and q is the momentum of the virtual phonon. The tensor $W^{\mu\nu}(p,q)$ is defined as the imaginary part of the virtual-photon–hadron forward-scattering amplitude, as illustrated in Fig. 1. Because of electromagnetic gauge invariance, the tensor $W^{\mu\nu}(p,q)$ can be decomposed as[2,5]

$$W^{\mu\nu}(p,q)=e_L^{\mu\nu}F_L(x_B,Q^2)+e_T^{\mu\nu}F_T(x_B,Q^2)\ , \tag{1}$$

where $Q^2=-q^2$, $x_B=Q^2/2p\cdot q$, and the invariant tensors $e_L^{\mu\nu}$ and $e_T^{\mu\nu}$ are defined as

$$e_L^{\mu\nu}=\frac{1}{2}\left[g^{\mu\nu}-\frac{q^\mu q^\nu}{q^2}\right],$$

$$e_T^{\mu\nu}=\frac{x_B}{p\cdot q}p^\mu p^\nu+\frac{1}{2p\cdot q}(p^\mu q^\nu+q^\mu p^\nu)-\tfrac{1}{2}g^{\mu\nu}\ . \tag{2}$$

The longitudinal and transverse structure functions $F_L(x_B,Q^2)$ and $F_T(x_B,Q^2)$ are related to the standard structure functions by

$$F_2(x_B,Q^2)=x_BF_T(x_B,Q^2)\ ,$$

$$F_1(x_B,Q^2)=\tfrac{1}{2}[F_T(x_B,Q^2)-F_L(x_B,Q^2)]\ .$$

To calculate the twist-4 corrections to these structure functions, one should calculate the twist-4 contributions to the tensor $W^{\mu\nu}(p,q)$, and then use Eq. (1) to extract the corresponding contributions to the longitudinal and transverse structure functions.

Before introducing our new method, let us study why the standard Feynman-diagram approach for calculating the twist-4 corrections is very complicated. In EFP's standard Feynman-diagram approach, they expand the virtual-phonon–hadron forward scattering amplitude in terms of Feynman diagrams, as shown in Fig. 2. At any given order of the strong coupling constant g, they include only diagrams whose strong quark-gluon interaction vertices can be met to the same point when the two photon-quark interaction vertices are shrunk to a single point. Such expansion is obviously a direct extension of OPE calculation. At any given twist, calculating the

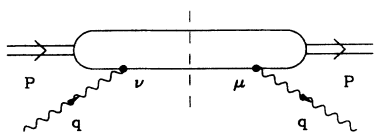

FIG. 1. The virtual-photon–hadron forward-scattering amplitude.

leading contribution to the hadron structure functions is to pick up the leading short-distance strong-interaction part from these Feynman diagrams (i.e., to calculate the corresponding coefficient function in OPE language). In EFP's approach, they give a consistent factorization scheme to separate the bottom photon-parton scattering parts from corresponding top target matrix elements. All bottom parts are well defined and calculable. After performing such a factorization, however, one will find a potential difficulty involved in such a approach. That is, the top parts of three diagrams in Fig. 2 are different from each other, and the individual bottom part *does not* conserve the electromagnetic gauge invariance. Because the short-distance coefficient functions and the long-distance target matrix elements should separately conserve gauge invariance, we should expect a nontrivial mixture of contributions to the coefficient functions from different diagrams in Fig. 2, and, hence, a possible distortion of the photon-parton scattering picture of the twist-4 short-distance contributions.

The key in EFP's approach is to use equations of motion to relate the two- and three-parton target matrix elements [the top parts of diagrams in Figs. 2(a) and 2(b)] to the four-parton target matrix element. After a long, clever, and very complicated derivation, EFP did find the gauge-invariant $1/Q^2$ corrections to the structure functions. Their result can be written as

$$F_L(x_B,Q^2)=\frac{4}{Q^2}T_1(x_B)+O\left[\frac{1}{Q^4}\right], \tag{3}$$

$$F_T(x_B,Q^2)=\frac{1}{Q^2}\left[4T_1(x_B)-x_B\int dx_2dx_1\frac{\delta(x_2-x_B)-\delta(x_1-x_B)}{x_2-x_1}T_2(x_2,x_1)\right]+O\left[\frac{1}{Q^4}\right]. \tag{4}$$

(For simplicity, we show only the leading $1/Q^2$ contribution without including the leading-twist contribution in the formulas of structure functions here. We shall consider only the limit of zero target mass in this paper. The dependence on target mass will not change our conclusion.) In this formula the x_1 and x_2 are light-cone momentum fractions of parton momenta k_1 and k_2, see Fig. 2, and T_1 and T_2 are the four-parton correlation functions. They are defined on the light-cone as

$$\begin{aligned}T_1(x_B)&=\frac{1}{4}\int\frac{d\lambda}{2\pi}e^{i\lambda x_B}\langle p|T\bar{\psi}(0)\gamma_\alpha\not{n}\gamma_\beta D_T^\alpha(0)D_T^\beta(\lambda)\psi(\lambda)|p\rangle\ ,\\ T_2(x_2,x_1)&=\frac{1}{4}\int\frac{d\lambda d\eta}{(2\pi)^2}e^{i\eta(x_2-x_1)}e^{i\lambda x_1}\langle p|T\bar{\psi}(0)\gamma_\alpha\not{n}\gamma_\beta D_T^\beta(\eta)D_T^\alpha(\eta)\psi(\lambda)|p\rangle\ ,\end{aligned} \tag{5}$$

where the $D_T^\alpha(\lambda)$ is the transverse component of the covariant derivative[5] and the λ is the light-cone coordinate. The final result of EFP is very compact, and depends only on one four-parton target matrix element. However, after mixing contributions from the two- and three-parton correlation functions with the four-parton correlation function, it is not clear if the twist-4 short-distance contributions have a simple parton-model interpretation.[5]

In EFP's approach, the mixing of the multiparton target matrix elements makes the calculation of high-twist contributions very nontrivial, and the mixing makes the parton picture unclear. The reason for this kind of mixing is actually due to the factorization procedure. The factorization procedure introduced by EFP is a consistent procedure to separate the spinor trace and the sum of Lorentz indices between the top and bottom parts. But this is not a procedure to completely factorize the short-distance interaction part from the long-distance part, because the top parts obtained after performing such a factorization still include some short-distance hard interac-

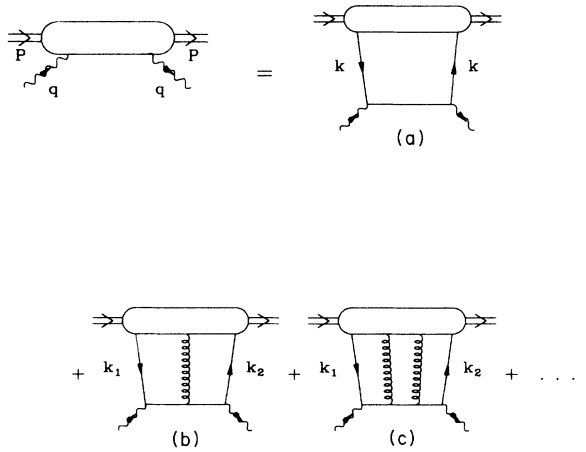

FIG. 2. Feynman-diagram expansion of the virtual-photon–hadron forward-scattering amplitude used in EFP's approach.

tion pieces. The key in our new method is to exclusively use the Feynman diagram technique to explicitly separate the short-distance interaction part from the corresponding long-distance matrix element order by order (*twist by twist*). To be able to pick up the short-distance contribution from a given Feynman diagram, we shall introduce a new physical concept—the special propagator, which is a part of a normal propagator, but *does not* propagate. Using the concept of special propagator, we find that the total twist-4 short-distance contributions to the hadron structure functions arise from the complete imaginary part of a photon-parton forward scattering amplitude, and, hence, they can be given a simple parton-model interpretation.

Understanding exactly how the lower-order diagram [e.g., one in Fig. 2(a)] gives high-twist contribution is the key to separate different-twist contributions of each diagram in Fig. 2. In the $N\cdot A=0$ gauge, the leading contribution from a diagram with n loop partons (those in Fig. 2) is to the twist-n short-distance coefficient function when we let all loop parton momenta entering the bottom part of the diagram be on-shell and collinear. The diagram can obviously give a high-twist contribution if the loop parton momenta entering the bottom part are not taken to be on shell and collinear. We find that for any diagram shown in Fig. 2, the effect due to the noncollinear components of loop momenta entering the bottom part of the diagram is to replace the gluon operators in the higher-order diagrams by corresponding covariant derivatives.[5] For example, the leading contribution due to the nonlinear component of loop momentum k entering the bottom part of the diagram in Fig. 2(a) is to replace the gluon operator in the top part of the diagram in Fig. 2(b) by corresponding covariant derivative. Similarly, the next-to-leading contribution from the diagram in Fig. 2(a) plus the leading contribution from the diagram in Fig. 2(b), due to the noncollinear components of loop parton momenta entering the bottom parts, is to replace the gluon operators in the top part of the diagram in Fig. 2(c) by corresponding covariant derivatives.

However, even all loop parton momenta entering the bottom part are set to be on shell and collinear, the diagram can still give higher-twist contributions. This is actually caused by two facts. One of them is that the loop propagators that are defined to be included into the top part of the diagram have the "contact" terms, which offer no space separation along the light-cone coordinate [see Eq. (14)]. The other is the existence of nonvanishing intrinsic transverse momenta of the loop propagators. By studying how the simplest diagram shown in Fig. 2(a) can give a high-twist contribution, as an example, one can see the existence of the above two facts and understand in general how a low-order diagram can give a high-twist contribution. After approximating the loop momentum k entering the bottom part to be xp, and parametrizing the virtual-photon momentum q as in Eq. (9), the bottom part of the diagram in Fig. 2(a) must be proportional to $\gamma\cdot n$ or $\gamma\cdot p$. When the term proportional to $\gamma\cdot n$ contracted with the top part, we get the normal leading twist-2 contribution. When the term proportional to $\gamma\cdot p$ contracted with the top part, we will get the high-twist contribution. As a definition, the top part includes the two loop propagators of momentum k. In terms of the general decomposition of momentum k in Eq. (6), it is clear that the collinear part of the loop momentum does not give the high-twist contribution because $\gamma\cdot(xp)\gamma\cdot p=0$. When $\gamma\cdot p$ contracted with the loop propagator $i\gamma\cdot k/k^2$, there are two possible nonvanishing terms. One of them is proportional to $i\gamma\cdot n/(2k\cdot n)$, which is indeed the "contact" term [see Eq. (14)] defined as the special propagator; and the other depends explicitly on k_T. Because of Eq. (15) it is clear that the second term can be combined with the first term to preserve the color gauge invariance. Because the contact term offers no space separation along the light-cone coordinates, the combination of a contact term and a directly connected quark-gluon vertex should be included into the bottom short-distance interaction part. From simple dimensional analysis, one can see that moving every one combination of a special propagator and a directly connected vertex is to move one unit of dimension [1/energy] from a top part to a corresponding bottom part. The new short-distance bottom part thus contributes to one twist higher structure functions. By moving two such combinations from the top to the bottom part, we can get the twist-4 contribution included in the diagram shown in Fig. 2(a).

In Sec. II, we shall show the existence of the contact term, and introduce a new concept—the special propagator. The special propagator is a propagator that does not propagate. It is defined to be equal to the contact term of a corresponding normal propagator. The special propagator offers no space separation along the light-cone coordinates of two interaction points connected by the propagator. Using the property of the special propagator, we shall introduce a method to separate the short-distance photon-parton hard interaction part from the long-distance target matrix elements. Using the method introduced in Sec. II, we shall give a complete list of technical steps to calculate the leading twist-4 contributions to the hadron structure functions in Sec. III. Following these technical steps, we shall compute the twist-4 contributions. For the completion, we shall also discuss the four-quark case which is much simpler than the quark-gluon case. Finally, in Sec. IV we shall summarize the physical concepts and new technique used in our new approach. We shall also discuss the possible extension of our method and discuss the possible application of this $1/Q^2$ corrections to the effective hadron structure functions of a big nucleus.

II. THE SPECIAL PROPAGATORS

In this section we shall show explicitly how a low-order diagram [e.g., one in Fig. 2(a)] can give the high-twist contribution. By introducing a new concept—the special propagator, we shall show how to separate the short-distance and long-distance contributions of a diagram. We then introduce a method to pick up the high-twist contribution from a low-order diagram *twist by twist.*

Introducing an auxiliary lightlike vector n, we fix the gauge as $n\cdot A=0$, where A is the gluon field. In terms of the auxiliary vector n, we may decompose any parton

momentum k as

$$k^\mu = xp^\mu + \frac{k^2+k_T^2}{2k\cdot n}n^\mu + k_T^\mu ,$$
$$\equiv \hat{k}^\mu + \frac{k^2}{2k\cdot n}n^\mu \tag{6}$$

where

$$p^2 = n^2 = p\cdot k_T = n\cdot k_T = 0, \quad \hat{k}^2 = 0 . \tag{7}$$

In terms of plus and minus notation,

$$k_+ = k\cdot n, \quad k_- = k\cdot\hat{p} , \tag{8}$$

where $\hat{p}_\mu = p_\mu / p\cdot n$. In Eq. (6), $x = k\cdot n / p\cdot n$ as the longitudinal-momentum fraction carried by a parton of momentum k in the infinite-momentum frame. We parametrize the virtual-photon momentum q as

$$q^\mu = -x_B p^\mu + \frac{Q^2}{2x_B p\cdot n}n^\mu . \tag{9}$$

It follows that $q^2 = -Q^2$ and $x_B = Q^2/2p\cdot q$.

Having the gauge and the frame fixed, we can write the leading photon-hadron forward scattering amplitude [the diagram in Fig. 2(a)] as

$$M_2^{\mu\nu} = \int \frac{d^4k}{(2\pi)^4}[\hat{S}^{\mu\nu}(k)\hat{T}(k)] , \tag{10}$$

where the subscript 2 indicates the process having two loop partons, the square brackets indicate the trace over spinor indices, $\hat{S}$ is a bottom part defined *not* to include the loop propagators of momentum k, and $\hat{T}$ is the corresponding top part given by

$$\hat{T}(k) = \int d^4z\, e^{ikz}\langle p|\bar{\psi}(0)\psi(z)|p\rangle . \tag{11}$$

Similarly, we can write down the amplitudes for the processes shown in Figs. 2(b) and 2(c) (see next section).

In principle, the imaginary part of the amplitude $M_2^{\mu\nu}$ given in Eq. (10) can give a contribution to the structure functions at any twist equal to or larger than two. The leading twist-2 contribution is obtained when the loop momentum k entering the bottom part $\hat{S}^{\mu\nu}(k)$ is equal to its collinear component. The diagram can give a high-twist contribution when the k in $\hat{S}^{\mu\nu}(k)$ has a nonlinear component. One can pick up the high-twist contribution due to the noncollinear component of the loop momentum entering the bottom part $\hat{S}^{\mu\nu}(k)$ by expanding the bottom at $k^\mu = xp^\mu$:

$$\hat{S}^{\mu\nu}(k) = \hat{S}^{\mu\nu}(xp) + \left.\frac{\partial\hat{S}^{\mu\nu}}{\partial k^\alpha}\right|_{k=xp}(k-xp)^\alpha + \frac{1}{2}\left.\frac{\partial^2\hat{S}^{\mu\nu}}{\partial k^\alpha\partial k^\beta}\right|_{k=xp} \times (k-xp)^\alpha(k-xp)^\beta + \cdots . \tag{12}$$

As we shall show in Sec. III, the effect of high-order terms in the above expansion is to replace the gluon field operators in the higher-order diagrams by the corresponding covariant derivatives. That is, the high-twist contribution due to the noncollinear component of k entering the bottom part can be easily taken care of.

The difficult part of calculating the high-twist contribution is to pick up the short-distance contribution from the top part $\hat{T}(k)$. Substituting Eq. (12) into (10), all high-order terms will contribute to high-twist structure functions. The treatment of these terms is straightforward and will be given in the next section. The first term, however, can give not only leading twist-2 contributions, but also high-twist contributions. To find the high-twist contribution from the first term is nontrivial. It is the main task of this section and includes all basic ideas involved in our new approach.

After performing the collinear expansion of the bottom part $\hat{S}$, every term in the expansion must be *proportional* to $\gamma\cdot n$ and/or $\gamma\cdot p$. Clearly, the $\hat{S}^{\mu\nu}(xp)$ [the first term in Eq. (12)] can be proportional to $\gamma\cdot n$ or $\gamma\cdot p$. When $\hat{S}^{\mu\nu}(xp)$ contracted with the top part $\hat{T}(k)$, the term proportional to $\gamma\cdot n$ gives the normal leading twist-2 contribution. As we shall show in the following paragraphs, the term proportional to $\gamma\cdot p$ results in the high-twist contribution. If we apply EFP's factorization scheme to separate the bottom part $\hat{S}^{\mu\nu}(xp)$ from the top part $\hat{T}(k)$, the target matrix element $[\hat{T}(k)\gamma\cdot p]$ will include a high-twist short-distance contribution. We then have the complicated mixing problem. What we shall do here is include all possible high-twist short-distance contributions into the bottom part first, and then apply EFP's factorization scheme to separate the short-distance bottom part at a given twist from corresponding long-distance top part.

To study how the target matrix element $\hat{T}(k)$ contracted with $\gamma\cdot p$ can give a high-twist *short-distance* contribution is to study $(i\gamma\cdot k/k^2)\gamma\cdot p$ and/or $\gamma\cdot p(i\gamma\cdot k/k^2)$. When $\hat{T}(k)$ is contracted with $\gamma\cdot p$, as shown in Fig. 3, it is clear that the collinear part of $\gamma\cdot k$ does not contribute because $\gamma\cdot(xp)\gamma\cdot p = 0$. In terms of the general decomposition of momentum k in Eq. (6), we find that (1) $[\hat{T}(k)\gamma\cdot p]$ will not be equal to zero if the loop parton has an intrinsic transverse momentum (i.e., $k_T \neq 0$); more importantly, (2) $[\hat{T}(k)\gamma\cdot p]$ does not vanish even though $k_T = 0$, because of the existence of a term $i\gamma\cdot n/(2k\cdot n)$ in the loop propagator $i\gamma\cdot k/k^2$. This term is the "contact" term that offers no space separation along the light-cone coordinate and plays a key role in our new approach.

The "contact" term of a normal propagator is a term that does not propagate along the light-cone coordinate. The existence of such a term in a normal propagator can be demonstrated by studying the light-cone coordinate dependence of a propagator of momentum k propagating from a vertex at light-cone coordinate $\lambda\cdot n$ to another vertex at $\eta\cdot n$. For example, for a quark propagator of momentum k,

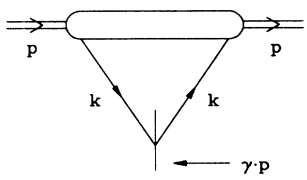

FIG. 3. The cut vertex to pick up the high-twist contribution.

$$F(k)=\frac{i\gamma\cdot k}{k^2}=\frac{i\gamma\cdot\hat{k}}{k^2}+\frac{i\gamma\cdot n}{2k\cdot n}\ , \tag{13}$$

we consider transformation

$$\frac{1}{2\pi}\int dk_- e^{-ik_-(\eta-\lambda)_+}\frac{i\gamma\cdot k}{k^2+i\epsilon}$$
$$=\delta(\eta_+-\lambda_+)\frac{i\gamma_+}{2k_+}+\theta(\eta_+-\lambda_+)\frac{\gamma\cdot\hat{k}}{2k_+}$$
$$\times e^{-i(k_T^2/2k_+)(\eta_+-\lambda_+)}\ , \tag{14}$$

where we have used the plus and minus notation defined in Eq. (8) for simplicity. The $\hat{k}$ in Eq. (14) is defined in Eq. (6) and is equal to the on-shell part of momentum k. Equation (14) shows clearly that every quark propagator has a contact term (the δ-function term). Similarly, as shown in Eq. (27), every gluon propagator has a contact term also. To identify the contact term, we introduce a new concept—the special propagator which is defined to be equal to the contact part of a normal propagator, and is symbolized by the normal propagator with a short bar [see, e.g., Fig. 4(a)]. For a normal quark propagator of momentum k, $F(k)=i\gamma\cdot k/k^2$, the corresponding special propagator is equal to $F_s(k)=i\gamma\cdot n/2k\cdot n$. Because this kind of contact term offers no space separation along the light-cone coordinate, clearly, such term in the loop propagators and the vertices (in the top matrix element) linking directly by these terms should be included into the short-distance photon-parton interaction part (coefficient function part). For example, the quark-gluon vertex and the special quark propagator in Fig. 4(a), which is just one part of the diagram shown in Fig. 3, should be included into the short-distance coefficient functions. The new top part is now a three-parton target matrix element. From the simple dimensional analysis, we conclude that because of the existence of the contact term in the loop propagator, $[\hat{T}(k)\gamma\cdot p]$ can give a high-twist short-distance contribution.

To see how the intrinsic transverse momentum k_T of the loop parton can result in the high-twist short-distance contribution, we again consider $[\hat{T}(k)\gamma\cdot p]$ shown in Fig. 3. After subtracting the diagram in Fig. 4(a) from the diagram in Fig. 3 (subtracting off the effect of the contact term), the left loop quark propagator of momentum k is now equal to $i\gamma\cdot\hat{k}/k^2$. It follows that the leftover top part is no longer equal to the two-parton matrix element defined in Eq. (11). When this leftover top part contracted with the $\gamma\cdot p$, we obtain

$$\left[\frac{i\gamma\cdot\hat{k}}{k^2}\right]\gamma\cdot p=\left[\frac{i\gamma\cdot k}{k^2}\right]\left[\frac{\gamma\cdot k\gamma\cdot\hat{k}}{k^2}\right]\gamma\cdot p$$
$$=\left[\frac{i\gamma\cdot k}{k^2}\right](k-xp)^\alpha(i\gamma_\alpha)\left[\frac{i\gamma\cdot n}{2k\cdot n}\right]\gamma\cdot p\ , \tag{15}$$

where we have used $\gamma\cdot\hat{k}\gamma\cdot\hat{k}=0$ and $\gamma\cdot p\gamma\cdot n\gamma\cdot p=2p\cdot n\gamma\cdot p$. From Eq. (15), clearly, the effect of the nonvanishing loop transverse momentum in the left quark propagator is equal to the diagram shown in Fig. 4(b). That is, the diagram in Fig. 3 is *equal* to the diagram in Fig. 4(a) plus the diagram in Fig. 4(b). As we shall show in the following paragraphs the two diagrams in Fig. 4 can be combined together. The effect of the second diagram is to replace the gluon field operator in the top part of the first diagram by corresponding covariant derivative. Therefore, we conclude that $[\hat{T}(k)\gamma\cdot p]$ shown in Fig. 3 gives a high-twist contribution.

We now show that the effect of the diagram in Fig. 4(b) is to replace the gluon field operator in the top part of the diagram in Fig. 4(a) by the corresponding covariant derivative. Using Eq. (15), we can write the contribution of diagrams in Fig. 4 as

$$M_a=\int\frac{d^4k}{(2\pi)^4}\frac{d^4k_1}{(2\pi)^4}[\hat{s}_\alpha(k,k_1)\hat{T}^\alpha(k,k_1)]\ ,$$
$$M_b=\int\frac{d^4k}{(2\pi)^4}[\hat{s}_\alpha(k,k)(k-xp)^\alpha\hat{T}^\alpha(k)]\ , \tag{16}$$

where $\hat{T}(k)$ is given in Eq. (11) and $\hat{T}^\alpha(k,k_1)$ is defined as

$$\hat{T}^\alpha(k,k_1)=\int d^4z\,d^4z_1 e^{i(k-k_1)z}e^{ik_1z_1}$$
$$\times\langle p|\bar{\psi}(0)(-g\tau^B A_B^\alpha(z))\psi(z_1)|p\rangle\ , \tag{17}$$

where B is a color index in the adjoint representation and τ^B is the color matrix and is normalized by $\mathrm{Tr}(\tau^B\tau^C)=\frac{1}{2}\delta^{BC}$. As in Eq. (17), we shall always include the color factor and the strong coupling constant of the bottom part of the diagram into the top matrix elements. Because the bottom parts $\hat{s}$ in Fig. 4 depend only on collinear components of the loop momenta (the special propagator depends only on the collinear component), we can rewrite Eq. (16) as

$$M_a=\int dx\,dx_1[\hat{s}_\alpha(xp,x_1p)\hat{T}^\alpha(x,x_1)]\ ,$$
$$M_b=\int dx[\hat{s}_\alpha(xp,xp)\hat{T}^\alpha(x)]\ , \tag{18}$$

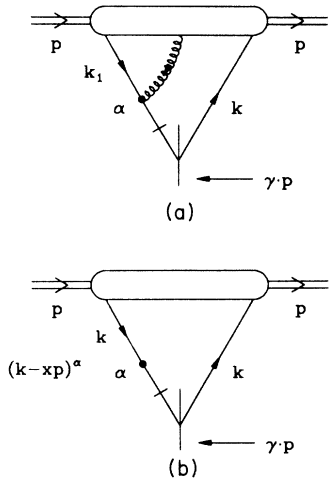

FIG. 4. Sample diagrams with the cut vertex shown in Fig. 3 that give the leading short-distance high-twist contribution.

where

$$\hat{T}^{\alpha}(x)=\int \frac{d^4k}{(2\pi)^4}\delta\left[x-\frac{k\cdot n}{p\cdot n}\right](k-xp)^{\alpha}\hat{T}(k)\ ,$$

$$\hat{T}^{\alpha}(x,x_1)=\int \frac{d^4k}{(2\pi)^4}\frac{d^4k_1}{(2\pi)^4}\delta\left[x-\frac{k\cdot n}{p\cdot n}\right]\times\delta\left[x_1-\frac{k_1\cdot n}{p\cdot n}\right]\hat{T}(k,k_1)\ . \tag{19}$$

By introducing a projecting operator $\omega^{\alpha}_{\alpha'}=g^{\alpha}_{\alpha'}-\hat{p}^{\alpha}n_{\alpha'}$, we find

$$(k-xp)^{\alpha}\hat{T}(k)=\omega^{\alpha}_{\alpha'}k^{\alpha'}\hat{T}(k)=\omega^{\alpha}_{\alpha'}\int d^4z\, e^{ikz}\langle p|\bar{\psi}(0)(i\partial^{\alpha'})\psi(z)|p\rangle\ . \tag{20}$$

Using Eq. (20), and the identity

$$\int \frac{d^4k}{(2\pi)^4}e^{ikz}\delta\left[x-\frac{k\cdot n}{p\cdot n}\right]=\int\frac{d\lambda}{2\pi}e^{i\lambda x}\delta^4\left[z-\frac{\lambda}{p\cdot n}n\right]\ , \tag{21}$$

where λ is a light-cone coordinate along the n direction and is scaled by a factor $1/p\cdot n$, we can rewrite Eq. (19) as

$$\hat{T}^{\alpha}(x)=\omega^{\alpha}_{\alpha'}\int\frac{d\lambda}{2\pi}e^{i\lambda x}\left\langle p\left|\bar{\psi}(0)(i\partial^{\alpha'})\psi\left[\frac{\lambda}{p\cdot n}\right]\right|p\right\rangle\ ,$$

$$\hat{T}^{\alpha}(x,x_1)=\int\frac{d\eta}{2\pi}\frac{d\lambda}{2\pi}e^{i\eta(x-x_1)}e^{i\lambda x_1}\left\langle p\left|\bar{\psi}(0)\left[-g\tau^B A^{\alpha}_B\left[\frac{\eta}{p\cdot n}\right]\right]\psi\left[\frac{\lambda}{p\cdot n}\right]\right|p\right\rangle\ . \tag{22}$$

Since

$$\omega^{\alpha}_{\alpha'}A^{\alpha'}_B\left[\frac{\eta}{p\cdot n}\right]=A^{\alpha}_B\left[\frac{\eta}{p\cdot n}\right]$$

and

$$1=\int dx_1\delta(x-x_1)=\int dx_1\int\frac{d\eta}{2\pi}e^{i\eta(x-x_1)}\ ,$$

M_a and M_b in Eq. (18) can be combined together as

$$M_a+M_b=\int dx\,dx_1[\hat{s}_{\alpha}(xp,x_1p)\omega^{\alpha}_{\alpha'}\hat{T}^{\alpha'}(x,x_1)]\ , \tag{23}$$

where $\hat{T}^{\alpha}(x,x_1)$ is, instead of Eq. (22), now given by

$$\hat{T}^{\alpha}(x,x_1)=\int\frac{d\eta}{2\pi}\frac{d\lambda}{2\pi}e^{i\eta(x-x_1)}e^{i\lambda x_1}\times\left\langle p\left|\bar{\psi}(0)D^{\alpha}\left[\frac{\eta}{p\cdot n}\right]\psi\left[\frac{\lambda}{p\cdot n}\right]\right|p\right\rangle\ , \tag{24}$$

where the D^{α} is a covariant derivative, and is given by $(i\partial^{\alpha}-g\tau^B A^{\alpha}_B)$.

Similarly, by applying the same technique to the right loop propagator of the diagram in Fig. 3, we find that the diagram in Fig. 3 is *equal* to the diagram in Fig. 5. The top part is a four-parton target matrix element given in Eq. (45), and the bottom part is the leading nontrivial high-twist short-distance contribution given by $[\hat{T}(k)\gamma\cdot p]$. Obviously, by applying our technique again between the new bottom and top parts, we can factorize out the short-distance contribution at even higher twists.

Based on the above example, we conclude that when $\gamma\cdot n$ is contracted with a loop quark-propagator of the top target matrix element, it picks up the leading-twist long-distance contribution of the matrix element;[7] when $\gamma\cdot p$ is contracted with a loop quark-propagator of the matrix element, it turns the loop propagator effectively into a special propagator and pulls down the special propagator and a directly connected quark-gluon vertex from the top matrix element into the corresponding bottom photon-parton interaction part to give the leading nontrivial high-twist short-distance contribution. The inclusion of one quark-gluon vertex and a special quark propagator into the bottom part increases the dimension of the bottom part by one unit of [1/energy], and thus makes the new bottom part contribute to the short-distance coefficient functions at one twist higher.

Because (1) every term in the collinear expanded bottom part is proportional to $\gamma\cdot n$ and/or $\gamma\cdot p$, (2) the $\gamma\cdot p$ turns the loop quark propagator effectively into a special propagator, and (3) the $\gamma\cdot n$ gives no effect on the special propagator ($\gamma\cdot n\gamma\cdot n=0$), we find that to obtain a higher-twist short-distance contribution from a lower-order diagram is to move a certain number of combinations of the special propagator and the connected vertex into the bottom part of the diagram; for example, the leading nontrivial high-twist short-distance contribution of the diagram in Fig. 2(a) is equal to the leading contribution of the diagram in Fig. 6(a). More detail will be given in the next section.

Now let us briefly discuss the special gluon propagator,

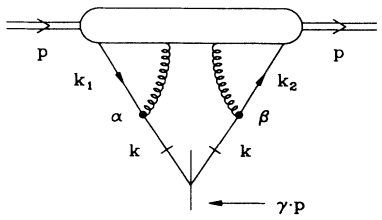

FIG. 5. The cut diagram that gives the leading short-distance twist-4 contribution.

$G_s^{\alpha\beta}(k)$. In our twist-4 calculation, we need only the one property of the special gluon propagator that the $G_s^{\alpha\beta}(k)$ is proportional to $n^\alpha n^\beta$. However, it will play an important role in a calculation of coefficient functions at even higher twists. In the light-cone gauge, the gluon propagator of momentum k is given by

$$G^{\alpha\beta}(k)=\frac{-i}{k^2}\Gamma^{\alpha\beta}(k) , \tag{25}$$

where the $\Gamma^{\alpha\beta}(k)$ is given by

$$\Gamma^{\alpha\beta}(k)=g^{\alpha\beta}-\frac{k^\alpha n^\beta+n^\alpha k^\beta}{k\cdot n} . \tag{26}$$

In terms of the general decomposition of parton momentum k given in Eq. (6), we can rewrite the gluon propagator as

$$G^{\alpha\beta}(k)=\frac{-i}{k^2}\Gamma^{\alpha\beta}(k)=\frac{-i}{k^2}\Gamma^{\alpha\beta}(\hat{k})+i\frac{n^\alpha n^\beta}{(k\cdot n)^2} . \tag{27}$$

By comparing Eq. (27) with Eq. (13) and carrying out the transformation shown in Eq. (14), we find that the special gluon propagator should be

$$G_s^{\alpha\beta}(k)=in^\alpha n^\beta/(k\cdot n)^2 ,$$

because it does not propagate. We also find that, similar to the role of the special quark propagator, the combination of the special gluon propagator and the connected vertex (trigluon vertex or gluon-quark-antiquark vertex) carries one *unit* of twist.

III. POWER CORRECTIONS TO THE STRUCTURE FUNCTIONS

In this section we shall use the method developed in the last section to separate the contributions from different twists, and to calculate the twist-4 contributions (i.e., the leading inverse-power corrections) to the hadron structure functions. After factorizing the short-distance interaction from corresponding long-distance physics, we find that the twist-4 short-distance interaction part can be expressed in terms of some simple photon-parton scattering processes. The long-distance part is given by a well-defined target matrix element.

To get complete twist-4 contributions, we should pick up all $1/Q^2$ contributions not only from diagrams shown in Fig. 2 but also from the four-quark process shown in Fig. 7(a). The treatment of this four-quark process is straightforward and will be given at the end of this section. The special treatment of quark-gluon process is the main task of this paper.

Our technical steps for picking up the complete $1/Q^2$ contributions from diagrams in Fig. 2 are (1) to find the $1/Q^2$ contribution caused by the noncollinear components of loop momenta entering the bottom parts (this step can be done by simply expanding the loop momenta in bottom parts at the values of their collinear components), (2) to show that the effect of all nonleading terms in the collinear expansion is to replace the gluon field operators in the top target matrix elements by corresponding covariant derivatives, (3) to show that when the leading terms in the expansion of the bottom parts are contracted with corresponding top parts, they give both leading-twist and high-twist contributions, (4) to show that after carefully separating the short-distance and long-distance contributions from the leading terms of lower-order diagrams, the high-twist contribution from the lower-order diagrams are indeed equal to the contribution of some higher-order diagrams not explicitly included in Fig. 2, (5) to show that the complete $1/Q^2$ short-distance contribution can be expressed in terms of some simple photon-parton scattering process, and finally, (6) to calculate all those short-distance photon-parton scattering processes to get complete twist-4 contribution.

Following our technical steps given above, we now show that the effect of all nonleading terms in the collinear expansion of lower-order bottom parts is to replace the gluon field operators in the higher-order top target matrix elements by corresponding covariant derivatives.[5] Similar to Eq. (10), we can write the leading photon-hadron forward scattering amplitudes from the diagrams shown in Figs. 2(b) and 2(c) as

$$M_3^{\mu\nu}=\int\frac{d^4k_2}{(2\pi)^4}\frac{d^4k_1}{(2\pi)^4}[\hat{S}_\alpha^{\mu\nu}(k_2,k_1)\hat{T}^\alpha(k_2,k_1)] , \tag{28}$$

$$M_4^{\mu\nu}=\int\frac{d^4k_2}{(2\pi)^4}\frac{d^4k}{(2\pi)^4}\frac{d^4k_1}{(2\pi)^4}\times[\hat{S}_{\alpha\beta}^{\mu\nu}(k_2,k,k_1)\hat{T}^{\alpha\beta}(k_2,k,k_1)] , \tag{29}$$

where the three-parton top matrix element $\hat{T}^\alpha(k_2,k_1)$ is defined in Eq. (17), and the four-parton top matrix element is given by

$$\hat{T}^{\alpha\beta}(k_2,k,k_1)=\int d^4z_2d^4z\,d^4z_1e^{i(k_2-k)z_2}e^{i(k-k_1)z}e^{ik_1z_1}\langle p|\bar{\psi}(0)(-g\tau^BA_B^\alpha(z_2))(-g\tau^CA_C^\beta(z))\psi(z_1)|p\rangle , \tag{30}$$

where we have included all color factors and strong coupling constants of the bottom part into the top part. To pick up the high-twist contributions caused by noncollinear components of loop momenta in the bottom parts, we expand the loop momenta in the bottom parts at the values of their collinear components. To pick up the twist-4 contribution, we expand $\hat{S}^{\mu\nu}(k)$ up to the second order shown in Eq. (12), and expand $\hat{S}_\alpha^{\mu\nu}(k_2,k_1)$ and $\hat{S}_{\alpha\beta}^{\mu\nu}(k_2,k,k_1)$ as

$$\begin{aligned}\hat{S}_\alpha^{\mu\nu}(k_2,k_1)=&\hat{S}_\alpha^{\mu\nu}(x_2p,x_1p)\\&+\frac{\partial\hat{S}_\alpha^{\mu\nu}}{\partial k_2^\beta}\bigg|_{k_2=x_2p,\,k_1=x_1p}(k_2-x_2p)^\beta\\&+\frac{\partial\hat{S}_\alpha^{\mu\nu}}{\partial k_1^\beta}\bigg|_{k_2=x_2p,\,k_1=x_1p}(k_1-x_1p)^\beta+\cdots ,\end{aligned} \tag{31}$$

$$\hat{S}^{\mu\nu}_{\alpha\beta}(k_2,k,k_1)=\hat{S}^{\mu\nu}_{\alpha\beta}(x_2p,xp,x_1p)+\cdots . \tag{32}$$

Using the identity

$$\frac{\partial}{\partial k^\alpha}\left[\frac{i}{\gamma\cdot k}\right]=\left\{\left[\frac{i}{\gamma\cdot k}\right](i\gamma_\alpha)\left[\frac{i}{\gamma\cdot k}\right]\right\} \tag{33}$$

and the definitions of the top and bottom parts, we find[5]

$$\left.\frac{\partial\hat{S}^{\mu\nu}}{\partial k^\alpha}\right|_{k=xp}=\hat{S}^{\mu\nu}_{\alpha}(xp,xp) ,$$

$$\left.\frac{1}{2}\frac{\partial^2\hat{S}^{\mu\nu}}{\partial k^\alpha\partial k^\beta}\right|_{k=xp}=\hat{S}^{\mu\nu}_{\alpha}(xp,xp,xp) ,$$

$$\left.\frac{\partial\hat{S}^{\mu\nu}_{\alpha}}{\partial k_2^\beta}\right|_{k_2=x_2p,\,k_1=x_1p}=\hat{S}^{\mu\nu}_{\alpha\beta}(x_2p,x_2p,x_1p) , \tag{34}$$

$$\left.\frac{\partial\hat{S}^{\mu\nu}_{\alpha}}{\partial k_1^\beta}\right|_{k_2=x_2p,\,k_1=x_1p}=\hat{S}^{\mu\nu}_{\alpha\beta}(x_2p,x_1p,x_1p) .$$

Using Eq. (34), we can rewrite the amplitudes as

$$M_2^{\mu\nu}=\int dx[\hat{S}^{\mu\nu}(xp)\hat{T}(x)]+\int dx[\hat{S}^{\mu\nu}_{\alpha}(xp,xp)\hat{T}^{\alpha}(x)]+\int dx[\hat{S}^{\mu\nu}_{\alpha\beta}(xp,xp,xp)\hat{T}^{\alpha\beta}(x)]+\cdots , \tag{35}$$

$$M_3^{\mu\nu}=\int dx_2dx_1[\hat{S}^{\mu\nu}_{\alpha}(x_2p,x_1p)\hat{T}^{\alpha}(x_2,x_1)]+\int dx_2dx_1[\hat{S}^{\mu\nu}_{\alpha\beta}(x_2p,x_2p,x_1p)\hat{T}^{\alpha\beta}_{2}(x_2,x_1)]$$

$$+\int dx_2dx_1[\hat{S}^{\mu\nu}_{\alpha\beta}(x_2p,x_1p,x_1p)\hat{T}^{\alpha\beta}_{1}(x_2,x_1)]+\cdots , \tag{36}$$

$$M_4^{\mu\nu}=\int dx_2dx\,dx_1[\hat{S}^{\mu\nu}_{\alpha\beta}(x_2p,xp,x_1p)\hat{T}^{\alpha\beta}(x_2,x,x_1)]+\cdots , \tag{37}$$

where $\hat{T}^{\alpha}(x)$ and $\hat{T}^{\alpha}(x_2,x_1)$ are given in Eq. (19) or (22), and

$$\hat{T}(x)=\int\frac{d^4k}{(2\pi)^4}\delta\left[x-\frac{k\cdot n}{p\cdot n}\right]\hat{T}(k) , \tag{38}$$

$$\hat{T}^{\alpha\beta}(x)=\int\frac{d^4k}{(2\pi)^4}\delta\left[x-\frac{k\cdot n}{p\cdot n}\right](k-xp)^\alpha(k-xp)^\beta\hat{T}(k) , \tag{39}$$

$$\hat{T}^{\alpha\beta}_{2}(x_2,x_1)=\int\frac{d^4k_2}{(2\pi)^4}\frac{d^4k_1}{(2\pi)^4}\delta\left[x_2-\frac{k_2\cdot n}{p\cdot n}\right]\delta\left[x_1-\frac{k_1\cdot n}{p\cdot n}\right](k_2-x_2p)^\beta\hat{T}^{\alpha}(k_2,k_1) , \tag{40}$$

$$\hat{T}^{\alpha\beta}_{1}(x_2,x_1)=\int\frac{d^4k_2}{(2\pi)^4}\frac{d^4k_1}{(2\pi)^4}\delta\left[x_2-\frac{k_2\cdot n}{p\cdot n}\right]\delta\left[x_1-\frac{k_1\cdot n}{p\cdot n}\right](k_1-x_1p)^\alpha\hat{T}^{\beta}(k_2,k_1) , \tag{41}$$

$$\hat{T}^{\alpha\beta}_{2}(x_2,x,x_1)=\int\frac{d^4k_2}{(2\pi)^4}\frac{d^4k}{(2\pi)^4}\frac{d^4k_1}{(2\pi)^4}\delta\left[x_2-\frac{k_2\cdot n}{p\cdot n}\right]\delta\left[x-\frac{k\cdot n}{p\cdot n}\right]\delta\left[x_1-\frac{k_1\cdot n}{p\cdot n}\right]\hat{T}^{\alpha\beta}(k_2,k,k_1) . \tag{42}$$

By introducing the projecting operator $\omega^\alpha_{\alpha'}$, using the identity given in Eq. (21), and following the derivation from Eq. (20) to Eq. (23), we find that the effect of the second term in Eq. (35) is to replace the gluon field operator in the first term in Eq. (36) by a corresponding covariant derivative, and the effect of the third term in Eq. (35) plus the second and third terms in Eq. (36) is to replace the gluon field operators in the leading term in Eq. (37) by corresponding covariant derivatives. Therefore, we have

$$M^{\mu\nu}=M_2^{\mu\nu}+M_3^{\mu\nu}+M_4^{\mu\nu}+\cdots$$

$$=\int dx[\hat{S}^{\mu\nu}(xp)\hat{T}(x)]+\int dx_2dx_1[\hat{S}^{\mu\nu}_{\alpha}(x_2p,x_1p)\omega^\alpha_{\alpha'}\hat{T}^{\alpha'}(x_2,x_1)]$$

$$+\int dx_2dx\,dx_1[\hat{S}^{\mu\nu}_{\alpha\beta}(x_2p,xp,x_1p)\omega^\alpha_{\alpha'}\omega^\beta_{\beta'}\hat{T}^{\alpha'\beta'}(x_2,x,x_1)]+\cdots , \tag{43}$$

where $\hat{T}^{\alpha}(x_2,x_1)$ is given in Eq. (24), and

$$\hat{T}(x)=\int \frac{d\lambda}{2\pi}e^{i\lambda x}\left\langle p\left|\bar{\psi}(0)\psi\left[\frac{\lambda}{p\cdot n}\right]\right|p\right\rangle , \tag{44}$$

$$\hat{T}^{\alpha\beta}(x_2,x,x_1)=\int \frac{d\omega}{2\pi}\frac{d\eta}{2\pi}\frac{d\lambda}{2\pi}e^{i\omega(x_2-x)}e^{i\eta(x-x_1)}e^{i\lambda x_1}\times\left\langle p\left|\bar{\psi}(0)D^{\alpha}\left[\frac{\omega}{p\cdot n}\right]D^{\beta}\left[\frac{\eta}{p\cdot n}\right]\psi\left[\frac{\lambda}{p\cdot n}\right]\right|p\right\rangle . \tag{45}$$

After taking care of the high-twist contribution caused by noncollinear components of loop parton momenta entering the bottom parts, we now calculate the possible high-twist contributions from the top parts $\hat{T}$, due to the contact terms and the nonvanishing intrinsic transverse components of loop parton momenta in the loop propagators. That is, we are going to find the possible twist-4 contribution from the first two terms in the right-hand side of Eq. (43).

As we discussed in the last section, the expanded bottom parts $\hat{S}^{\mu\nu}$ have typically two terms, one of them is proportional to $\gamma\cdot n$, and the other proportional to $\gamma\cdot p$. We will get higher-twist short-distance contribution if the top part $\hat{T}$ contracted with the $\gamma\cdot p$ term. This is because $\gamma\cdot p$ contracted with one-loop quark propagator will pull a special propagator and a directly connected quark-gluon vertex into the bottom *short-distance* part, and increase the bottom part by one unit of dimension [1/energy], and thus one unit of twist. The new top *long-distance* part has then an extra operator—a covariant derivative. Therefore, the way to obtain twist-4 short-distance contribution from $\int dx[\hat{S}^{\mu\nu}(xp)\hat{T}(x)]$ is to move *two* combinations of the special quark propagator and the connected quark-gluon vertex from $\hat{T}(x)$ into the bottom part $\hat{S}^{\mu\nu}(xp)$ [see diagrams shown in Figs. 6(a) and 6(c)]; and to obtain twist-4 short-distance contribution from $\int dx_2dx_1[\hat{S}^{\mu\nu}_{\alpha}(x_2p,x_1p)\omega^{\alpha}_{\alpha'}\hat{T}^{\alpha'}(x_2,x_1)]$ is to move *one* combination of the special quark propagator and the connected quark-gluon vertex from $\hat{T}^{\alpha'}(x_2,x_1)$ into the corresponding bottom part [see diagrams shown in Fig. 6(b)]. Because of the special gluon propagator, in principle, the diagrams shown in Figs. 6(d) and 7(b) can also give twist-4 short-distance contribution. The diagrams shown in Fig. 7(b) actually supplement to the four-quark process shown in Fig. 7(a).

We find that the diagrams shown in Figs. 6(c) and 6(d) vanish. The diagrams in Fig. 6(c) vanish because they have a common factor $\gamma\cdot n\,\gamma_T\gamma\cdot n=0$, where the two $\gamma\cdot n$ are from two special quark propagators and the middle γ_T is from the quark-gluon vertex, where we have used a fact that the γ matrix at the vertex cannot have a "$-$" component due to the projection operator ω, i.e., due to the gauge that we choose. The diagrams in Fig. 6(d) vanish because they have a common factor $\gamma\cdot n\,\gamma\cdot n=0$, where one $\gamma\cdot n$ is from a quark-gluon vertex connected to a special gluon propagator and the other is from a special quark propagator or from the cut of a quark line. That is, only four diagrams shown in Figs. 2(c), 6(a), and 6(b) give nonvanishing twist-4 short-distance contributions to hadron scattering functions. The four-quark process will be discussed later.

We now show explicitly how the nonvanishing diagrams shown in Figs. 6(a) and 6(b) can be *derived* from the first two terms in the right-hand side of Eq. (43).

In the expanded bottom parts $\hat{S}^{\mu\nu}$, every quark propagator has two terms. One of them is proportional to $\gamma\cdot n$ and the other is proportional to $\gamma\cdot p$. For example, the quark propagator in $\hat{S}^{\mu\nu}(xp)$ is proportional to $(x-x_B)\gamma\cdot p+(Q^2/2x_Bp\cdot n)\gamma\cdot n$. Therefore, every expanded bottom part should be proportional to $\gamma\cdot n$ and/or $\gamma\cdot p$. To get the imaginary part of the forward scattering amplitude is to cut the quark propagator in the expanded bottom parts.[5] We find that the cut quark propagator is proportional to $\gamma\cdot n$. For example, when we cut the propagator in $\hat{S}^{\mu\nu}(xp)$, we have

$$\delta((xp+q)^2)=(x_B/Q^2)\delta(x-x_B) .$$

Because of the $\delta(x-x_B)$, we have $\gamma\cdot(xp+q)\propto\gamma\cdot n$, and thus the cut quark propagator is proportional to $\gamma\cdot n$.

After taking a cut through the quark propagator in $\hat{S}^{\mu\nu}(xp)$, we find that the bottom part is now proportional $\gamma^{\mu}\gamma\cdot n\gamma^{\nu}$. The superscripts μ and ν can be any one of the following combinations, $\hat{p}^{\mu}\hat{p}^{\nu}$, $\hat{p}^{\mu}n^{\nu}$, $n^{\mu}\hat{p}^{\nu}$, $n^{\mu}n^{\nu}$, and $d^{\mu\nu}=\hat{p}^{\mu}n^{\nu}+n^{\mu}\hat{p}^{\nu}-g^{\mu\nu}$, where $d^{\mu\nu}$ is a transverse tensor. Because of the properties of the $\hat{p}$ and n given in Eq. (7), it is clear that the cut bottom part can be only proportional to $\gamma\cdot n$ when the indices μ and ν are transverse, or proportional to $\gamma\cdot p$ when the indices are both equal to $-$ (e.g., $\gamma^{\mu}=\gamma^{-}=\gamma\cdot\hat{p}$). Because of the existence of a term proportional to $\gamma\cdot p$, the first term in Eq. (43) will give a high-twist contribution. Since the $\gamma\cdot p$ is directly contracted with both loop propagators in this case, the $\gamma\cdot p$ will pull *two* special propagators and *two* directly connected quark-gluon vertices from the top part $\hat{T}(x)$ into the bottom part $\hat{S}^{\mu\nu}(xp)$, as shown in Fig. 5. Because the special propagator is proportional to $\gamma\cdot n$, and $\gamma\cdot n\,\gamma\cdot n=0$, we find the twist-4 contribution from the first term in Eq. (43):

$$\int dx[\hat{S}^{\mu\nu}(xp)\hat{T}(x)]\Big|_{\text{twist 4}}=\int dx_2dx\,dx_1[\hat{S}^{\mu\nu}_{\alpha\beta}(x_2p,xp,x_1p)_a\omega^{\alpha}_{\alpha'}\omega^{\beta}_{\beta'}\hat{T}^{\alpha'\beta'}(x_2,x,x_1)]_{\text{twist 4}} , \tag{46}$$

which is the leading contribution of the diagram shown in Fig. 6(a). The top part $\hat{T}^{\alpha\beta}(x_2,x,x_1)$ is defined in Eq. (45), and the short-distance bottom part $\hat{S}^{\mu\nu}_{\alpha\beta}(x_2p,xp,x_1p)_a$ is given by the leading contribution of the bottom part of the diagram in Fig. 6(a).

It is also straightforward to get the diagrams shown in Fig. 6(b) from the second term in Eq. (43). Notice that the second term in Eq. (43) does not vanish only when the

γ_α in the bottom part $\hat{S}_\alpha^{\mu\nu}(x_2p,x_1p)$ is equal to its transverse component. The γ_α cannot be equal to $\gamma\cdot\hat{p}$ because of the projection operator $\omega_{\alpha'}^{\alpha}$. The term vanishes when the γ_α is equal to $\gamma\cdot n$ because one of the propagators in the bottom part has to be proportional to $\gamma\cdot n$ after taking the cut. It follows that one of the two-loop quark propagators of the top part $\hat{T}^{\alpha}(x_2,x_1)$ has to be next to $\gamma\cdot\hat{p}$. Therefore, a special propagator and a directly connected quark-gluon vertex should be included into the bottom short-distance part. From simple dimensional analysis, the leading nonvanishing piece of the second term in Eq. (43) contributes to the twist-4 structure functions. It is actually given by the leading contribution of the diagrams in Fig. 6(b). That is, after taking the cut,

$$\int dx_2dx_1[\hat{S}_\alpha^{\mu\nu}(x_2p,x_1p)\omega_{\alpha'}^{\alpha}\hat{T}^{\alpha'}(x_2,x_1)]|_{\text{twist 4}}$$
$$=\int dx_2dx\,dx_1[\,\hat{S}_{\alpha\beta}^{\mu\nu}(x_2p,xp,x_1p)_b\omega_{\alpha'}^{\alpha}\omega_{\beta'}^{\beta}$$
$$\times\hat{T}^{\alpha'\beta'}(x_2,x,x_1)]\,, \tag{47}$$

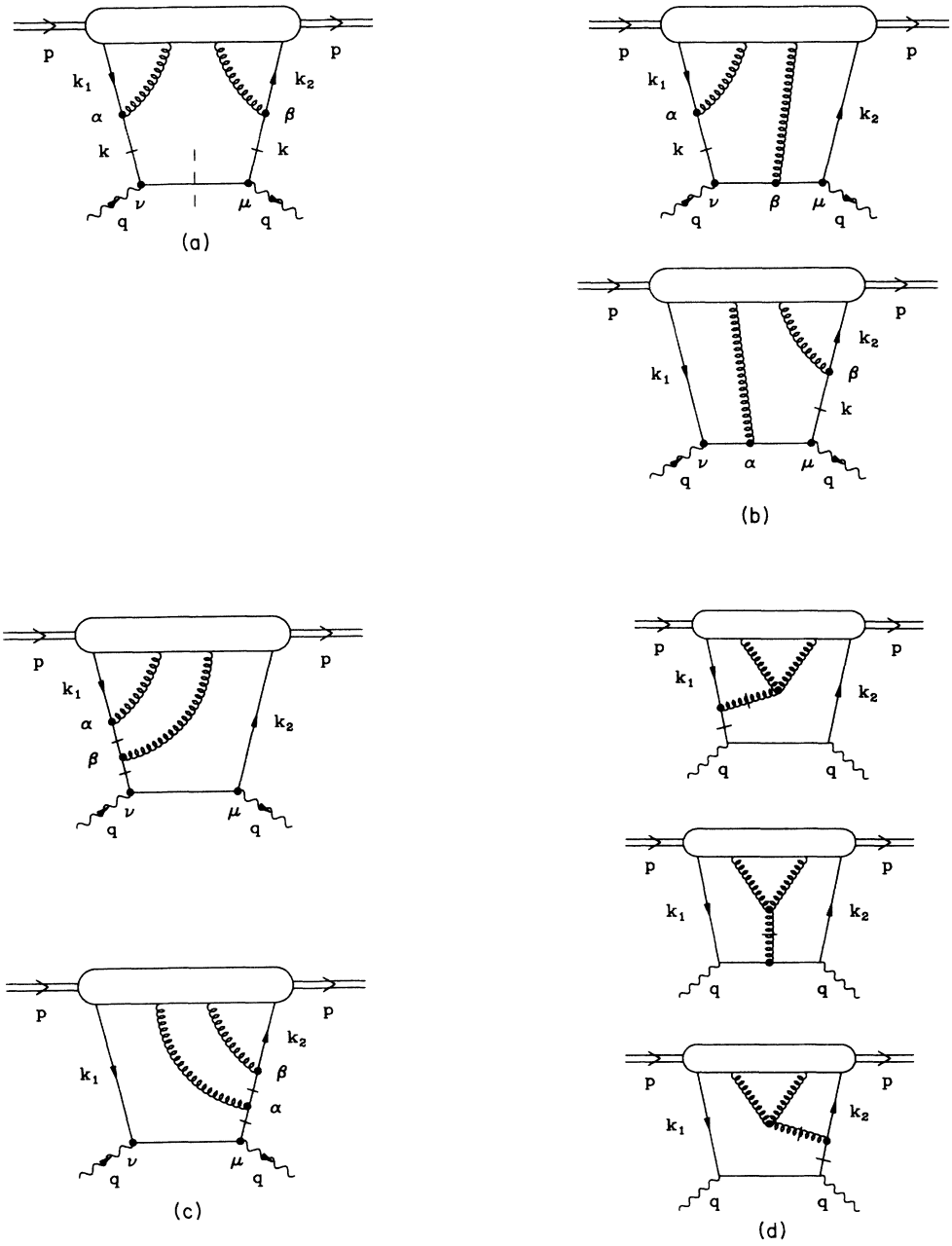

FIG. 6. A complete set of two-quark–two-gluon Feynman diagrams with special propagators that contribute to leading short-distance twist-4 coefficient functions.

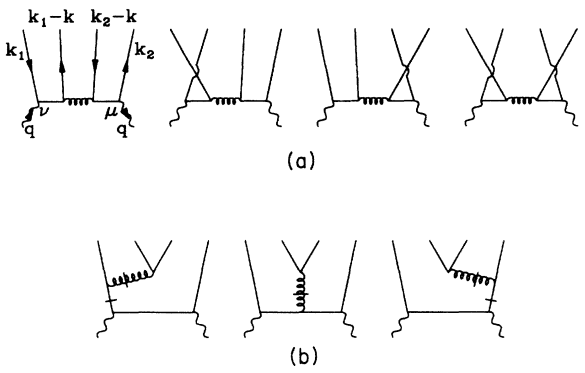

FIG. 7. A complete set of four-quark Feynman diagrams that contribute to leading short-distance twist-4 coefficient functions.

where the top part $\hat{T}^{\alpha\beta}(x_2,x,x_1)$ is given in Eq. (45), and the short-distance bottom part $\hat{S}^{\mu\nu}_{\alpha\beta}(x_2p,xp,x_1p)_b$ is given by the leading contribution of the bottom parts of the diagrams in Fig. 6(b).

We can now combine all nonvanishing twist-4 short-distance contributions together by substituting Eqs. (46) and (47) into Eq. (43),

$$M^{\mu\nu}|_{\text{twist 4}}=\int dx_1dx\,dx_1[\,\hat{S}^{\mu\nu}_{\alpha\beta}(x_2p,xp,x_1p)\omega^{\alpha}_{\alpha'}\omega^{\beta}_{\beta'}\times\hat{T}^{\alpha'\beta'}(x_2,x,x_1)]_{\text{twist 4}}\,, \tag{48}$$

where the short-distance bottom part $\hat{S}^{\mu\nu}_{\alpha\beta}(x_2p,xp,x_1p)$ now includes all four bottom parts of the diagrams shown in Figs. 2(c), 6(a), and 6(b).

Based on our derivation of the twist-4 short-distance contribution, it is clear that the complete twist-4 short-distance contributions (not including four-quark process) arise only from the two-photon, two-quark, and two-gluon tree diagrams [shown in Figs. 2(c) and 6], which form a complete set of Feynman diagrams of the photon-quark-gluon forward scattering amplitude at order of g^2; and, the corresponding long-distance part is given by one target matrix element of a well-defined operator [given in Eq. (45)]. Hence, there is no mixing problem, and as we shall show shortly, the short-distance part and long-distance part conserve the gauge invariance explicitly. We shall now apply EFP's factorization scheme to separate the spinor trace and Lorentz sum between the top and the bottom parts, and to pick up the twist-4 short-distance contribution.

To decouple the spinor trace over top and bottom parts, we expand the top part $\hat{T}^{\alpha\beta}(x_2,x,x_1)$ in the standard basis of gamma matrices. For the case of massless quarks, we obtain

$$\hat{T}^{\alpha\beta}(x_2,x,x_1)=\gamma_\rho C^{\rho\alpha\beta}(x_2,x,x_1)+\gamma_5\gamma_\rho\tilde{C}^{\rho\alpha\beta}(x_2,x,x_1)\,. \tag{49}$$

Substituting Eq. (49) into Eq. (48), we find

$$M^{\mu\nu}|_{\text{twist 4}}=\int dx_2dx\,dx_1\{S^{\mu\nu}_{\alpha\beta\rho}(x_2p,xp,x_1p)\omega^{\alpha}_{\alpha'}\omega^{\beta}_{\beta'}C^{\rho\alpha'\beta'}(x_2,x,x_1)+\tilde{S}^{\mu\nu}_{\alpha\beta\rho}(x_2p,xp,x_1p)\omega^{\alpha}_{\alpha'}\omega^{\beta}_{\beta'}\tilde{C}^{\rho\alpha'\beta'}(x_2,x,x_1)\}_{\text{twist 4}}\,, \tag{50}$$

where

$$\begin{aligned}
&S^{\mu\nu}_{\alpha\beta\rho}(x_2p,xp,x_1p)=[\hat{S}^{\mu\nu}_{\alpha\beta}(x_2p,xp,x_1p)\gamma_\rho]\,,\\
&C^{\rho\alpha\beta}(x_2,x,x_1)=\tfrac{1}{4}[\gamma^\rho\hat{T}^{\alpha\beta}(x_2,x,x_1)]\,,\\
&\tilde{S}^{\mu\nu}_{\alpha\beta\rho}(x_2p,xp,x_1p)=[\hat{S}^{\mu\nu}_{\alpha\beta}(x_2p,xp,x_1p)\gamma_5\gamma_\rho]\,,\\
&\tilde{C}^{\rho\alpha\beta}(x_2,x,x_1)=\tfrac{1}{4}[\gamma^\rho\gamma_5\hat{T}^{\alpha\beta}(x_2,x,x_1)]\,.
\end{aligned} \tag{51}$$

Equation (50) shows clearly that the spinor trace has been completely decoupled between top and bottom parts.

To have complete factorization, we need to decouple all the sums of Lorentz indices in Eq. (50). In general, the target matrix element $C^{\rho\alpha\beta}(x_2,x,x_1)$ can be decomposed into terms proportional to combinations of vectors p and n and a symmetric transverse tensor d, and $\tilde{C}^{\rho\alpha\beta}(x_2,x,x_1)$ into terms proportional to combinations of vectors p and n and an antisymmetric transverse tensor ϵ defined below. Obviously, there are a lot of terms. However, notice that (1) any term with three n vectors (e.g., $n^\rho n^\alpha n^\beta$) will give a zero result when it is contracted with the bottom hard-scattering part, (2) any term proportional to n^ρ will give either contribution higher than twist 4 or zero, (3) without n^ρ, any term with two n vectors (e.g., $p^\rho n^\alpha n^\beta$) will not contribute, and (4) any term proportional to p^α or p^β vanishes because the projection operator ω. We find a very simple effective result

$$\begin{aligned}
&C^{\rho\alpha\beta}(x_2,x,x_1)=C(x_2,x,x_1)p^\rho d^{\alpha\beta}\,,\\
&\tilde{C}^{\rho\alpha\beta}(x_2,x,x_1)=i\tilde{C}(x_2,x,x_1)p^\rho\epsilon^{\alpha\beta}\,,
\end{aligned} \tag{52}$$

where

$$d^{\alpha\beta}=\hat{p}^{\alpha}n^{\beta}+n^{\alpha}\hat{p}^{\beta}-g^{\alpha\beta},\quad \epsilon^{\alpha\beta}=\epsilon^{\alpha\beta\rho\sigma}\hat{p}_\rho n_\sigma\,. \tag{53}$$

Notice that the $d^{\alpha\beta}$ and $\epsilon^{\alpha\beta}$ defined here are the same as those defined by EFP up to a sign. Using Eq. (52) and Eq. (50), we obtain a factorized form of the hadronic tensor $W^{\mu\nu}$ contributing to the twist-4 hadron structure functions

$$\begin{aligned}
W^{\mu\nu}|_{\text{twist 4}}&=\frac{1}{2i}\text{Disc}(M^{\mu\nu}|_{\text{twist 4}})\\
&=\int dx_2dx\,dx_1(\sigma^{\mu\nu}(x_2,x,x_1)C(x_2,x,x_1)+\tilde{\sigma}^{\mu\nu}(x_2,x,x_1)\tilde{C}(x_2,x,x_1))\,,
\end{aligned} \tag{54}$$

where

$$\sigma^{\mu\nu}(x_2,x,x_1)=\frac{1}{2i}\mathrm{Disc}\{d^{\alpha\beta}[\hat{S}^{\mu\nu}_{\alpha\beta}(x_2p,xp,x_1p)\gamma\cdot p]\}\ ,$$
$$\sigma^{\mu\nu}(x_2,x,x_1)=\frac{1}{2i}\mathrm{Disc}\{i\epsilon^{\alpha\beta}[\hat{S}^{\mu\nu}_{\alpha\beta}(x_2p,xp,x_1p)\gamma_5\gamma\cdot p]\}\ , \tag{55}$$

$$C(x_2,x,x_1)=\int\frac{d\omega}{2\pi}\frac{d\eta}{2\pi}\frac{d\lambda}{2\pi}e^{i\omega(x_2-x)}e^{i\eta(x-x_1)}e^{i\lambda x_1}\frac{1}{8}d^{\alpha\beta}\langle p|T(\bar{\psi}(0)\gamma\cdot nD_\alpha(\omega)D_\beta(\eta)\psi(\lambda))|p\rangle\ ,$$
$$\tilde{C}(x_2,x,x_1)=\int\frac{d\omega}{2\pi}\frac{d\eta}{2\pi}\frac{d\lambda}{2\pi}e^{i\omega(x_2-x)}e^{i\eta(x-x_1)}e^{i\lambda x_1}\frac{1}{8i}\epsilon^{\alpha\beta}\langle p|T(\bar{\psi}(0)\gamma\cdot n\gamma_5D_\alpha(\omega)D_\beta(\eta)\psi(\lambda))|p\rangle\ . \tag{56}$$

This is our final factorized formula for calculating the leading twist-4 or $1/Q^2$ power correction to the hadron structure functions. It is clear that the short-distance part is given by the complete imaginary part of a photon-parton forward scattering amplitude, the target matrix elements derived here show explicitly gauge invariance if one inserts the line integrals of the gluon field between parton fields in the target matrix elements. The upper and lower limits of any line integral inserted between two parton fields are equal to the light-cone coordinates of these two parton fields, respectively. Therefore, in our new derivation, the parton-model interpretation of the twist-4 short-distance contribution and the underlying gauge invariance are manifestly preserved.

We shall now calculate the $\sigma^{\mu\nu}(x_2,x,x_1)$ and $\tilde{\sigma}^{\mu\nu}(x_2,x,x_1)$ from the short-distance photon-parton interactions. Using the same normalization of EFP, and our definition of special quark propagators, we calculate all four photon-parton Feynman diagrams [shown in Figs. 2(c), 6(a), and 6(b)] with all possible cuts, and we find

$$\sigma^{\mu\nu}(x_2,x,x_1)=\frac{8}{Q^2}(e_T^{\mu\nu}+e_L^{\mu\nu})\delta(x-x_B)-\frac{2x_B}{Q^2}e_T^{\mu\nu}\left[\frac{\delta(x_2-x_B)-\delta(x_1-x_B)}{x_2-x_1}\right],$$
$$\tilde{\sigma}^{\mu\nu}(x_2,x,x_1)=-\frac{8}{Q^2}(e_T^{\mu\nu}+e_L^{\mu\nu})\delta(x-x_B)-\frac{2x_B}{Q^2}e_T^{\mu\nu}\left[\frac{\delta(x_2-x_B)-\delta(x_1-x_B)}{x_2-x_1}\right], \tag{57}$$

where $e_L^{\mu\nu}$ and $e_T^{\mu\nu}$ are given in Eq. (2). In Eq. (57) the color factor and strong coupling constant g are included into the target matrix elements by definition. For simplicity, we also absorb the quark charge e_q^2 into the target matrix elements. As we expect, $\sigma^{\mu\nu}$ and $\tilde{\sigma}^{\mu\nu}$ in Eq. (57) show explicit electromagnetic gauge invariance. Introducing a new definition of target matrix elements

$$C_L(x_2,x,x_1)=C(x_2,x,x_1)-\tilde{C}(x_2,x,x_1)$$
$$C_R(x_2,x,x_1)=C(x_2,x,x_1)+\tilde{C}(x_2,x,x_1)\ , \tag{58}$$

we find the leading inverse-power correction to the hadronic tensor $W^{\mu\nu}(x_B,Q^2)$ as

$$W^{\mu\nu}(x_B,Q^2)|_{\text{twist 4}}=\frac{8}{Q^2}(e_T^{\mu\nu}+e_L^{\mu\nu})\int dx\,\delta(x-x_B)\int dx_1dx_2C_L(x_2,x,x_1)$$
$$-\frac{2x_B}{Q^2}e_T^{\mu\nu}\int dx_1dx_2\left[\frac{\delta(x_2-x_B)-\delta(x_1-x_B)}{x_2-x_1}\right]\int dx\,C_R(x_2,x,x_1)\ . \tag{59}$$

[Here the sum over quark flavor has been assumed to be absorbed into the target matrix elements $C_L(x_2,x,x_1)$ and $C_R(x_2,x,x_1)$.] Comparing the above result with Eq. (1), we obtain the corresponding twist-4 correction to the structure functions:

$$F_L(x_B,Q^2)=\frac{8}{Q^2}\int dx\,\delta(x-x_B)\int dx_1dx_2C_L(x_2,x,x_1)\ , \tag{60}$$

$$F_T(x_B,Q^2)=\frac{8}{Q^2}\int dx\,\delta(x-x_B)\int dx_1dx_2C_L(x_2,x,x_1)-\frac{2x_B}{Q^2}\int dx_1dx_2\left[\frac{\delta(x_2-x_B)-\delta(x_1-x_B)}{x_2-x_1}\right]\int dx\,C_R(x_2,x,x_1)\ . \tag{61}$$

This final result is exactly the same as the result of EFP, shown in Eq. (3), if we define

$$T_1(x)=2\int dx_1 dx_2 C_L(x_2,x,x_1)\ ,$$
$$T_2(x_2,x_1)=2\int dx\ C_R(x_2,x,x_1)\ , \tag{62}$$

see Eqs. (6.43) and (6.44) of EFP.[5] Therefore, we can conclude[8] that by introducing the special propagators to separate short-distance and long-distance contributions at a given twist, we obtain the same leading inverse-power correction to the hadronic structure functions with the gauge invariance and parton-model interpretation manifestly preserved.

For completeness, we include the leading inverse-power corrections from the four-quark process (shown in Fig. 7). The diagrams shown in Fig. 7(b) actually vanish for the same reason that the diagrams in Fig. 6(d) vanish. The diagrams in Fig. 7(a) have been widely discussed. This process contributes to the twist-4 and even higher-twist structure functions. To pick up the twist-4 contributions, we expand the loop momenta in the bottom part at the values equal to their collinear components first, then use EFP's factorization scheme to separate the spinor trace and Lorentz sums between the bottom part and the top part. We get the same result as that obtained by EFP. We quote the result below:[5]

$$W_q^{\mu\nu}(x_B,Q^2)|_{\text{twist 4}}=e_T^{\mu\nu}\int dx_2 dx\ dx_1(\sigma_q(x_2,x,x_1)C_q(x_2,x,x_1)+\bar{\sigma}_q(x_2,x,x_1)\tilde{C}_q(x_2,x,x_1))\ , \tag{63}$$

where subscript q stands for the four-quark process, and the four-quark target matrix elements are given by

$$C_q(x_2,x,x_1)=\int\frac{d\omega}{2\pi}\frac{d\eta}{2\pi}\frac{d\lambda}{2\pi}e^{i\omega(x_2-x)}e^{i\eta(x-x_1)}e^{i\lambda x_1}\tfrac{1}{16}g^2\langle p|T\{[\bar{\psi}(0)\gamma\cdot n\tau^B\psi(\omega)][\bar{\psi}(\eta)\gamma\cdot n\tau^B\psi(\lambda)]\}|p\rangle\ ,$$
$$\tilde{C}_q(x_2,x,x_1)=\int\frac{d\omega}{2\pi}\frac{d\eta}{2\pi}\frac{d\lambda}{2\pi}e^{i\omega(x_2-x)}e^{i\eta(x-x_1)}e^{i\lambda x_1}\tfrac{1}{16}g^2\langle p|T\{[\bar{\psi}(0)\gamma\cdot n\gamma_5\tau^B\psi(\omega)][\bar{\psi}(\eta)\gamma\cdot n\gamma_5\tau^B\psi(\lambda)]\}|p\rangle\ . \tag{64}$$

The coefficient functions $\sigma_q(x_2,x,x_1)$ and $\bar{\sigma}_q(x_2,x,x_1)$ are[3,5]

$$\sigma_q(x_2,x,x_1)=\frac{x_B}{4Q^2}(\Delta(y_2,y_1,x)+\Delta(x_2,x_1,x)-\Delta(y_2,x_1,x)-\Delta(x_2,y_1,x))\ , \tag{65}$$

where

$$\Delta(x_2,x,x_1)=\frac{1}{x_2-x_1}\left[\frac{\delta(x_2-x_B)-\delta(x-x_B)}{x_2-x}-\frac{\delta(x_1-x_B)-\delta(x-x_B)}{x_1-x}\right],\quad y_1=x-x_1,\quad y_2=x-x_2\ , \tag{66}$$

and

$$\bar{\sigma}_q(x_2,x,x_1)=\sigma_q(x_2,x,x_1)\ . \tag{67}$$

Equations (58) and (63) are our final results for the leading $1/Q^2$ power corrections to the hadron structure functions.

IV. DISCUSSION

We have presented a new method for calculating the twist-4 contributions to the hadron structure functions. As expected, the result of our calculation reproduces the well-known inverse-power corrections to hadron structure functions. However, this new method leads to a clear space-time picture of the twist-4 short-distance contributions, and enables us to separate the different twist short-distance contribution from a given Feynman diagram. This new approach makes manifest the preservation of the underlying gauge invariance, and gives a simple parton-model interpretation of the twist-4 short-distance contributions. The use of the special propagators results in a significant reduction in labor relative to past calculations of higher-twist contributions. In this section we shall summarize the new method for calculating high-twist short-distance contributions, and discuss other possible applications of the space-time picture of the twist-4 effect. We shall also discuss the possible test of such $1/Q^2$ corrections to the effective parton structure functions in a big nucleus.

Our new method is based on the space-time picture of twist-4 short-distance contributions. The concept of a special propagator is a key to isolate the short-distance effect from the remaining long-distance target matrix elements. The special propagator not only picks up the "contact" piece of a normal propagator, but also links the effects of the intrinsic transverse components of the loop momenta to the covariant derivatives in the target matrix element to make the color gauge invariant manifest. In summary, we have the following rules for calculating the high-twist contribution to hadron structure functions: (1) to find all possible tree Feynman diagrams of a photon-parton forward scattering amplitude with the number of partons being equal to the number of the twist, and all coupling constants and the color factor being included into corresponding target matrix elements; (2) to replace all propagators, which will not be shrunk to a point as one shrinks the two photon-quark vertices together, by corresponding special propagators; (3) to factorize all spinor and Lorentz indices between the photon-parton processes and corresponding target matrix elements by following EFP's procedure; (4) to calculate all these tree photon-parton diagrams to obtain the short-distance contributions, as do the contributions to

hadron structure functions.

A remark is in order on the usage of such special propagators. Normally, we do not have to worry about the gauge invariance if we include and calculate *all* Feynman diagrams of a physical process at any given order of coupling constant (e.g., the complete imaginary part of a photon-parton forward scattering amplitude in this paper). However, the question here is if the replacement of the special propagators preserves gauge invariance property of the process, i.e., if the vertex involving a vector boson (photon or gluon) and quarks with special propagators still preserves the Ward identity such as

$$(k'-k)_\mu[F(k')\Gamma^\mu(k',k)F(k)]=-[F(k')-F(k)]\ , \quad (68)$$

where $F(k)$ and $\Gamma^\mu(k',k)$ are fermion propagator (quark propagator) and vertex function, respectively. The answer is *yes* in our calculation of the high-twist short-distance contributions. This can be demonstrated by considering the typical diagram shown in Fig. 8. From the vertex of quark and vector boson (wave line) in Fig. 8, we obtain the left-hand side of Eq. (68),

$$(k'-k)_\mu\left[\frac{\gamma\cdot k'}{k'^2}\gamma^\mu\frac{\gamma\cdot n}{2k\cdot n}\right]=-\left[\frac{\gamma\cdot k'}{k'^2}\frac{\gamma\cdot k\,\gamma\cdot n}{2k\cdot n}-\frac{\gamma\cdot n}{2k\cdot n}\right], \quad (69)$$

and the right-hand side of Eq. (68):

$$-\left[\frac{\gamma\cdot k'}{k'^2}-\frac{\gamma\cdot n}{2k\cdot n}\right]. \quad (70)$$

To have Eq. (68) satisfied, we need to show that $\gamma\cdot k\,\gamma\cdot n/2k\cdot n$ in the expression of left-hand side is equal to one. In general, $\gamma\cdot k\,\gamma\cdot n/2k\cdot n$ is not necessarily equal to one. However, in the calculations of the short-distance contributions at a given twist, it is always effectively equal to one for the following reason. When calculating a real diagram, see the typical diagram shown in Fig. 8, we need to multiply $\gamma_\alpha\gamma\cdot k_1$ to the right side of $\gamma\cdot k\,\gamma\cdot n/2k\cdot n$. As we discussed earlier, in the gauge we choose, the γ_α must be equal to γ_T or $\gamma\cdot n$. In the collinear expanded bottom part, $\gamma\cdot k_1$ is equal to $\gamma\cdot x_1 p$. Using $\gamma\cdot p\,\gamma\cdot n\,\gamma\cdot p=2p\cdot n\,\gamma\cdot p$, we conclude that $\gamma\cdot k\,\gamma\cdot n/2k\cdot n$ is effectively equal to one in the calculation of the complete diagrams. Therefore, the replacement of the special fermion propagator will not break the gauge invariance of the corresponding physical process. Our explicit calculation in the twist-4 case supports clearly this conclusion. Similarly, we find that the Ward identity involving the three gluon vertex and special gluon propagators is also satisfied in the leading high-twist calculation.

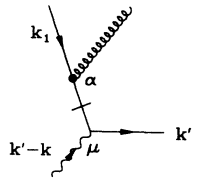

FIG. 8. A sample diagram used to show that the special propagator conserves the graphical Ward identity.

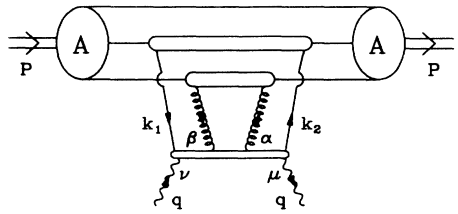

FIG. 9. A possible process, deep-inelastic lepton-nucleus scattering, that may test the short-distance twist-4 contribution.

We shall now discuss the possible test of the leading inverse-power corrections to the effective hadron structure functions. The experimental test of such $1/Q^2$ inverse-power corrections is difficult because of lack of knowledge of the multiparton target matrix elements, or multiparton correlation functions. However, in the rest of this paper, we shall suggest a possibility to test the effect of such inverse-power corrections in effective hadron structure functions of a big *nucleus*.

In the infinite-momentum frame, we view the target nucleus as a collection of uncorrelated nucleons with *weakly* correlated sea distributions.[9] The parton structure functions in a nucleus can then be approximated as a sum of parton structure functions of individual nucleons inside the nucleus plus a correction term due to the weakly correlated sea distributions. To estimate the correction term, we should calculate the interaction involving partons from two or more nucleons. The leading contribution clearly comes from the recombination effect involving two nucleons,[9,10] which contributes a correction to the leading-twist structure functions. But, because the leading twist component of this effect is calculated and included in the parton evolution equations, and because of the lack of knowledge of input structure function at a given Q_0^2 needed when solving the evolution equations, it is difficult to make precision test of this recombination effect. However, if we assume the gluon and quark in this four-parton twist-4 process are from two *different* nucleons as shown in Fig. 9, and take the limits $k_2\to k_1$, we find that the target matrix element $C(x_2,x,x_1)$ in Eq. (56) can be decoupled into the product of a quark number density of one nucleon, a gluon number density of another nucleon, and a correlation function to have these two partons at the same impact parameter, and $\tilde{C}(x_2,x,x_1)$ in Eq. (56) is zero. In this special case, the leading inverse-

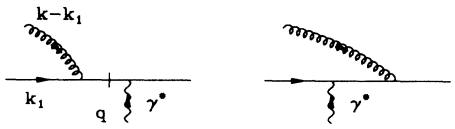

FIG. 10. The "real" photon-parton scattering process that contributes to leading twist-4 coefficient functions.

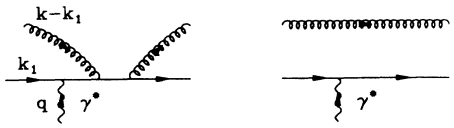

FIG. 11. The "interference" photon-parton scattering process that contributes to leading twist-4 coefficient functions.

power correction that we have just calculated in this paper can be related to the leading-twist single-parton number densities of different nucleons. The hard-interaction part $\sigma^{\mu\nu}$ in Eq. (57) can be then understood as a hard interaction between the virtual photon and a quark in the presence of a gluon. The correction to the effective nuclear structure functions due to this special leading twist-4 contribution can be evaluated without going through the complication of *input* structure functions. Therefore, at a given Q_0^2, the precise behavior of this particular leading twist-4 contribution to the effective structure functions of a big nucleus could give us some better knowledge about the effective *input* nuclear parton structure functions needed to solve the modified evolution equations to get the effective nuclear structure function, including recombination effects at any given large Q^2. In addition, because of the small-Q^2 dependence of both experimental data of the European Muon Collaboration effect[11] and theoretical prediction,[9] the precise behavior of this special leading inverse-power correction is even more interesting.

To understand the behavior of this special power correction, we go back to the hard-interaction part of this power correction in Eq. (57). The $\sigma^{\mu\nu}$ in Eq. (57) has two terms. The first term comes from a real physical process (shown in Fig. 10) after subtracting the lower-twist effect, which is included in the lower-twist structure function or included in the modified evolution equations of the structure functions. This process gives a positive-definite contribution to the effective parton structure functions in a big nucleus. The second term is equal to

$$-\frac{2x_B}{Q^2}e_T^{\mu\nu}\left[\frac{\delta(x_2-x_B)-\delta(x_1-x_B)}{x_2-x_1}\right]_{x_2\to x_1} = -\frac{2x_B}{Q^2}e_T^{\mu\nu}\delta'(x_1-x_B)\,, \quad (71)$$

and is from the interference between the amplitudes of order g^2 and of order g^0 shown in Fig. 11. This interference can only happen when the quark and gluon from two different nucleons are at the same impact parameter in a *big* nucleus, and the momentum fraction carried out by the quark or gluon should be small[9] so that $1/xp \geq L_{\rm eff}m/p$, where $L_{\rm eff}$ is the effective distance between two nucleons inside a nucleus. After taking into account the shape of parton number densities as a function of momentum fraction x, we find that the contribution of the interference term is always negative. Therefore, we have an interesting physical picture of this inverse-power correction. At a given value of x_B, if the first term in Eq. (61) is larger than the second term, we have an antishadowing effect; otherwise, we have a shadowing effect. The detailed analysis of this application will be the subject of another work.

ACKNOWLEDGMENTS

This work was supported by the U.S. National Science Foundation, Grant No. PHY89-08495 and by the U.S. Department of Energy, Division of High Energy Physics, Contract No. W-31-109-ENG-38. The author thanks G. Bodwin, J. C. Collins, R. K. Ellis, and A. H. Mueller for helpful discussions, and especially thanks E. L. Berger for a critical reading of the manuscript.

*Present address.

[1]R. P. Feynman, *Photon-Hadron Interactions* (Benjamin, New York, 1972); J. Kogut and L. Susskind, Phys. Rep. **8**, 76 (1973).

[2]For a general review, see E. Reya, Phys. Rep. **68**, 195 (1981); A. H. Mueller, *ibid.* **73**, 237 (1981); G. Altarelli, *ibid.* **81**, 1 (1982).

[3]A. De Rújula, H. Georgi, and H. D. Politzer, Ann. Phys. (N.Y.) **103**, 315 (1977); H. D. Politzer, Nucl. Phys. **B172**, 349 (1980); S. P. Luttrell and S. Wada, *ibid.* **B197**, 290 (1982); S. Wada, *ibid.* **B202**, 201 (1982); S. J. Brodsky, E. L. Berger, and G. P. Lepage, in *Proceedings of the Workshop on Drell-Yan Processes,* Batavia, Illinois, 1982 (Fermilab, Batavia, 1983), p. 187; references quoted by authors of Refs. 4–6.

[4]R. L. Jaffe and M. Soldate, Phys. Lett. **105B**, 467 (1981); Phys. Rev. D **26**, 49 (1982).

[5]R. K. Ellis, W. Furmanski, and R. Petronzio, Nucl. Phys. **B207**, 1 (1982); **B212**, 29 (1983).

[6]R. L. Jaffe, Nucl. Phys. **B229**, 205 (1983).

[7]G. Curci, W. Furmanski, and R. Petronzio, Nucl. Phys. **B175**, 27 (1980).

[8]J. L. Miramontes and J. Sánchez Guillén gave a similar conclusion with a different definition of the special propagator in Santiago Report No. USFT/20 (unpublished), which was quoted in Phys. Rev. D **30**, 46 (1984).

[9]J. Qiu, Nucl. Phys. **B291**, 746 (1987); E. L. Berger and J. Qiu, in *Nuclear Chromodynamics,* proceeding of the Topical Conference, Argonne, Illinois, 1988, edited by J. Qiu and D. Sivers (World Scientific, Singapore, 1988).

[10]A. H. Mueller and J. Qiu, Nucl. Phys. **B268**, 427 (1986); L. V. Gribov, E. M. Levin, and M. G. Ryskin, Phys. Rep. **100**, 1 (1983).

[11]J. Ashman *et al.*, Phys. Lett. B **202**, 603 (1988).